

Tunable magnetic orders in $UAu_{1-x}Sb_2$

Wen Zhang(张文), Qiu-Yun Chen(陈秋云), Dong-Hua Xie(谢东华), Yi Liu(刘毅), Shi-Yong Tan(谭世勇), Wei Feng(冯卫), Xie-Gang Zhu(朱燮刚), Qun-Qing Hao(郝群庆), Yun Zhang(张云), Li-Zhu Luo(罗丽珠), Xin-Chun Lai(赖新春)

Citation: Chin. Phys. B . 2019, 28(1): 017102. **doi:** 10.1088/1674-1056/28/1/017102
Journal homepage: http://cpb.iphy.ac.cn; http://iopscience.iop.org/cpb

What follows is a list of articles you may be interested in

Kosterlitz-Thouless transition, spectral property and magnetic moment for a two-dot structure with level difference

Yong-Chen Xiong(熊永臣), Wang-Huai Zhou(周望怀), Jun Zhang(张俊), Nan Nan(南楠)

Chin. Phys. B . 2017, 26(6): 067501. **doi:** 10.1088/1674-1056/26/6/067501

Growth and characterization of $CaCu_3Ru_4O_{12}$ single crystal

Wang Rong-Juan, Zhu Yuan-Yuan, Wang Li, Liu Yong, Shi Jing, Xiong Rui, Wang Jun-Feng

Chin. Phys. B . 2015, 24(9): 097501. **doi:** 10.1088/1674-1056/24/9/097501

Quantum phase transition and Coulomb blockade effect in triangular quantum dots with interdot capacitive and tunnel couplings

Xiong Yong-Chen, Wang Wei-Zhong, Yang Jun-Tao, Huang Hai-Ming

Chin. Phys. B . 2015, 24(2): 027501. **doi:** 10.1088/1674-1056/24/2/027501

Charge oscillation and many-body effect in triangular quantum dots

Xiong Yong-Chen, Wang Wei-Zhong

Chin. Phys. B . 2012, 21(11): 117501. **doi:** 10.1088/1674-1056/21/11/117501

Tunable magnetic orders in $UAu_{1-x}Sb_2$*

Wen Zhang(张文), Qiu-Yun Chen(陈秋云), Dong-Hua Xie(谢东华), Yi Liu(刘毅), Shi-Yong Tan(谭世勇), Wei Feng(冯卫), Xie-Gang Zhu(朱燮刚), Qun-Qing Hao(郝群庆), Yun Zhang(张云), Li-Zhu Luo(罗丽珠), and Xin-Chun Lai(赖新春)†

Science and Technology on Surface Physics and Chemistry Laboratory, Mianyang 621908, *China*

(Received 4 September 2018; revised manuscript received 7 November 2018; published online 12 December 2018)

Two nonstoichiometric $UAu_{1-x}Sb_2$ ($x = 0.25$, 0.1) single crystals are successfully synthesized using a flux method, and their physical properties are comprehensively studied by measuring the dc-magnetization and electrical resistivity. Evidence for at least three magnetic phases is found in these samples. In zero field, both samples undergo an antiferromagnetic transition at a relatively high temperature, and with further cooling they pass through another antiferromagnetic phase, before reaching a ferromagnetic ground state. Furthermore, the magnetic order can be tuned by varying the site occupation of Au. Such a tunable magnetic order may provide an opportunity for exploring the potential quantum critical behavior in this system.

Keywords: tunable magnetic order, metamagenetic transitions, $UAu_{1-x}Sb_2$

PACS: 75.30.Mb, 75.20.Hr, 71.27.+a **DOI:** 10.1088/1674-1056/28/1/017102

1. Introduction

In heavy-fermion (HF) systems, the various unusual physical properties, such as unconventional superconductivity, non-Fermi liquid behavior, tunable magnetic order, and hidden order arise from the subtle interplay between the f electrons and the conduction electrons.[1–5] The relative strength of the Kondo effect and Ruderman–Kittel–Kasuya–Yosida (RKKY) interaction can be easily changed by chemical doping x, pressure P, or magnetic field H, which gives rise to these exotic properties.[6–9] Uranium-based compounds provide an ideal platform to study the interplay between 5f orbitals and conduction electrons. Among them, the uranium-based ternary compounds UTX_2 (T = transition metal, X = pnictogen) are excellent target materials for studying these interesting physical properties, which can be tuned by varying the transition metal atom or the site occupation.[10–15] Rich magnetic properties in this family have been found, where the compounds with T = Co, Cu, Ag, and Au are reported to display ferromagnetic order, while those with T = Ni, Ru, and Pd are antiferromagnetic.[10,11]

One important point to be understood in this system is the magnetic transition behavior tuned by the site occupation of the transition metal. Previous studies found that nonstoichiometric $UT_{1-x}Sb_2$ single crystals such as $UNi_{0.5}Sb_2$,[12,13] $UCo_{0.5}Sb_2$,[14] $UCu_{0.9}Sb_2$,[15] and $UPd_{0.6}Sb_2$ [16] show some significantly different properties from the stoichiometric compounds. The stoichiometric compound USb_2 undergoes an antiferromagnetic transition at 203 K, with no other magnetic transitions at lower temperature,[17] and $UAuSb_2$ likely undergoes two magnetic transitions, a ferromagnetic one at T_C = 31 K and a possible antiferromagnetic transition at 43 K.[18] While $UAu_{0.8}Sb_2$ shows an antiferromagnetic transition at 71 K, another antiferromagnetic transition at 34 K, and a ferromagnetic transition at 10 K.[19] From these studies, it is obvious that Au doped into USb_2 has a close relationship with the magnetic transition behavior. However, these data are still not enough to obtain the universal laws to understand the relationship between the chemical doping and magnetic behavior, and more studies of different nonstoichiometric compounds $UT_{1-x}Sb_2$ are needed. Another important goal is to explore the potential quantum critical behavior in this system. The $UAu_{1-x}Sb_2$ is a good platform for studying the magnetic transition and the potential quantum critical behavior due to dramatically different magnetic states by varying the composition of Au. Thus there is still a lot of work to be done on the nonstoichiometric $UAu_{1-x}Sb_2$ single crystals.

In this paper, we successfully synthesize two nonstoichiometric $UAu_{1-x}Sb_2$ ($x = 0.25$, 0.1) single crystals by using a flux method and present a detailed study of their physical properties by measuring the dc-magnetization and electrical resistivity. At zero field, three magnetic phases are evident by magnetization and electrical resistivity measurements: a high temperature antiferromagnetic phase, a phase with both ferromagnetic component and antiferromagnetic component at intermediate temperatures, and a low temperature ferromagnetic phase. With an external field applied along the c axis, two metamagnetic transitions occur. Furthermore, the magnetic order can be tuned by varying the occupation of the Au site. The AFM transition temperature is significantly increased with the

*Project supported by the National Natural Science Foundation of China (Grant Nos. 11874330, 11504342, 11504341, and U1630248), the National Key R&D Program of China (Grant No. 2017YFA0303104), and the Science Challenge Project, China (Grant No. TZ2016004).

†Corresponding author. E-mail: laixinchun@caep.cn

© 2019 Chinese Physical Society and IOP Publishing Ltd

occupation of Au site decreasing, while the FM transition temperature is suppressed and vanishes in the stoichiometric USb_2 compound, which suggests that there is a possible critical point between $x = 1$ and 0.25. Our study on $UAu_{1-x}Sb_2$ single crystals may shed new light on understanding the magnetic behaviors and exploring the quantum critical point of these uranium-based ternary compounds.

2. Experiment

$UAu_{1-x}Sb_2$ single crystals were grown using a self-flux method.[19] U (99.9%), Au (99.999%), and Sb (99.9999%) were combined in an appropriate ratio and placed in an alumina crucible. The crucible was sealed in an evacuated silica tube, heated up to 1150 °C and held at this temperature for 24 h before being cooled down to 1050 °C over 1 h and slowly cooled down to 700 °C. The excess Sb flux was removed by centrifuging and plate-like crystals were mechanically separated from the crucible. The typical dimensions of the crystals are about 4 mm×4 mm×2 mm.

The chemical compositions were determined on the freshly cleaved plane with an energy dispersive x-ray spectrometer (EDS). To tune more and less occupation of Au site in $UAu_{1-x}Sb_2$, samples with starting compositions of U : Au : Sb = 1 : 4.5 : 14 and U : Au : Sb = 1 : 2 : 14 are used to obtain the $x = 0.1$ and 0.25 $UAu_{1-x}Sb_2$ single crystals, respectively, compared with that of 1 : 3.5 : 14 for our previous study on $UAu_{0.8}Sb_2$.[17]

3. Results and discussion

The EDS analysis on the starting composition of U : Au : Sb = 1 : 4.5 : 14 (U, 25.3%; Au, 23.1%; Sb, 51.6%) yields that its chemical composition is around $UAu_{0.9}Sb_2$, while $UAu_{0.75}Sb_2$ is for the other starting composition of U : Au : Sb = 1 : 2 : 14 (U, 26.4%; Au, 20.1%; Sb, 53.5%). Figure 1(a) shows the as-grown $UAu_{0.9}Sb_2$ single crystal sample. Figure 1(b) shows the scanning electron microscope (SEM) image of the freshly cleaved $UAu_{0.9}Sb_2$ single crystal, and the corresponding EDS results verify Au doped into the single crystal as shown in Fig. 1(c).

First, we measure the systematic magnetization and electrical resistivity on $UAu_{0.9}Sb_2$ and construct a field-temperature phase diagram with the field applied along the c-axis. Figure 2(a) displays the temperature dependence of dc-magnetization $M(T)$ of $UAu_{0.9}Sb_2$. Above 110 K, $M(T)$ can be fitted by a modified Curie–Weiss expression

$$\chi = \chi_0 + \frac{C}{T - \theta_p}, \tag{1}$$

where $C = N\mu_B^2\mu_{eff}^2/(3k_B)$, giving an effective moment of $\mu_{eff} = 3.51\ \mu_B$/U and a Curie–Weiss temperature of $\theta_p =$ 61.8 K. The μ_{eff} values are reduced compared with the effective magnetic moments of the free U^{4+} ions and U^{3+} ions ($\mu_{eff} = 3.58\ \mu_B$/U and 3.62 μ_B/U, respectively). The value of θ_p is positive along the c-axis, indicating the presence of ferromagnetic exchange interactions. The magnetization increases with temperature decreasing, and a broad peak can be observed at $T_{N1} = 59$ K, which likely corresponds to an antiferromagnetic magnetic transition. A dramatic peak can be observed at 43 K. With further reducing temperature, splitting of the zero-field cooled (ZFC) and field-cooled (FC) curves occurs at 37 K, indicating another antiferromagnetic transition and the onset of ferromagnetic component. At the lowest temperature, the increase of the magnetization indicates a possible ferromagnetic ground state. Figure 2(b) shows the temperature dependence of the dc-magnetization measured in the FC modes with different fields applied parallel to the c axis. Below 1.5 T, a kink or a peak feature can be observed around 59 K, which may correspond to the antiferromagnetic magnetic transition, and the transition temperature decreases slightly with field increasing. A sharp increase is found at lower temperature, which may correspond to a ferromagnetic transition. At 1.5 T and 1.75 T, the magnetization continues to increase and reaches a saturation level, which suggests a ferromagnetic transition.

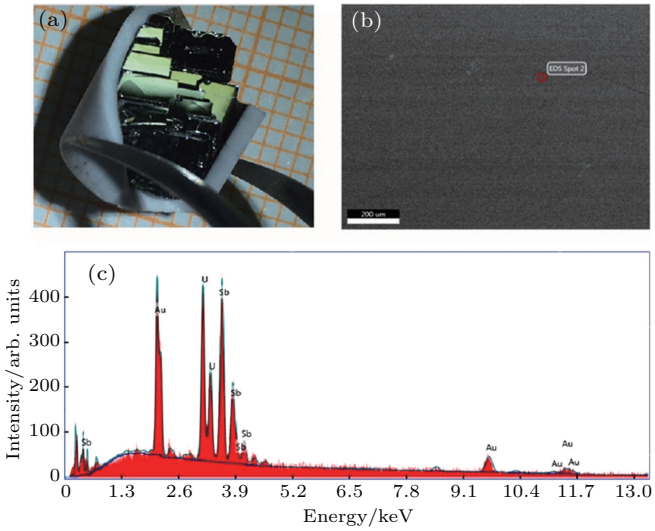


Fig. 1. (a) Image of as-grown $UAu_{0.9}Sb_2$ single crystal, (b) SEM image of freshly cleaved $UAu_{0.9}Sb_2$ single crystal, and (c) EDS results of $UAu_{0.9}Sb_2$ single crystal.

Figure 2(c) shows the temperature dependence of the electrical resistivity of $UAu_{0.9}Sb_2$ single crystal. The resistivity increases with decreasing temperature, and reaches a maximum value at about 65 K, which is slightly higher than the T_{N1} value derived from $M(T)$. In the paramagnetic state, above 100 K, the resistivity follows a logarithmic behavior

$$\rho(T) = \rho' - c_k \ln T, \tag{2}$$

where ρ' is a temperature independent term. As displayed in the inset, this expression can describe the higher temperature

data, indicating the presence of significant Kondo scattering. The cooling down and warming up resistivity curves show an obvious hysteresis from 48 K down to 34 K, revealing a first order transition at these intermediate temperatures. This is consistent with the broad peak in the $M(T)$ curves shown in Fig. 2(a). Figure 2(d) shows the temperature dependence of the resistivity measured in the FC modes with different fields applied parallel to the c axis. At the intermediate temperatures, the resistivity curves each show a sharp decrease, which is in line with the sharp increase in the magnetization curves shown in Fig. 2(b). The maximum temperature in the resistivity curve around T_{N1} slightly increases with magnetic field increasing, which may be due to the increased FM transition temperature at the intermediate temperatures.

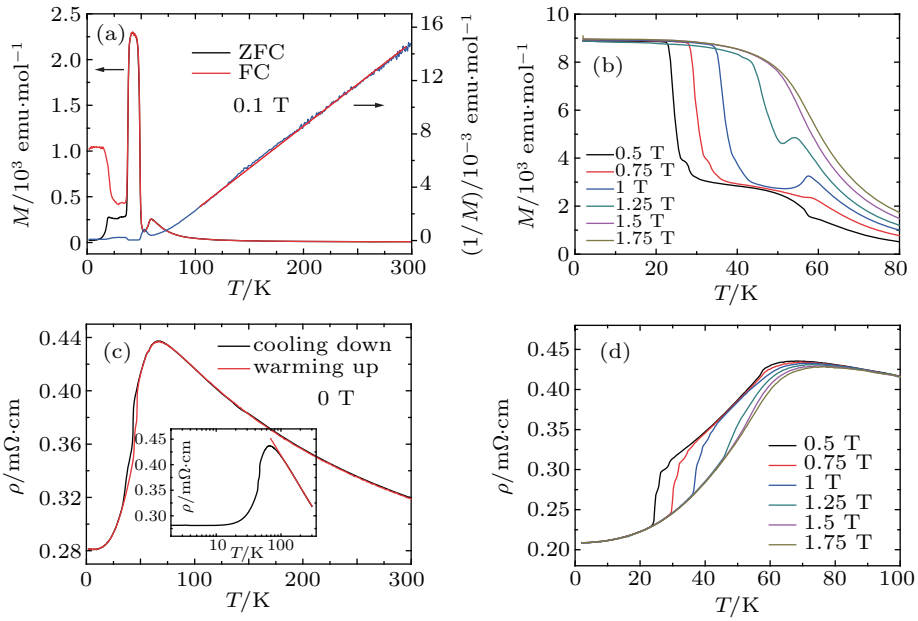


Fig. 2. Plots of dc-magnetization and electrical resistivity of $UAu_{0.9}Sb_2$ single crystal, showing (a) temperature dependence of dc-magnetization $M(T)$ (left-hand scale) and inverse dc-magnetization (right-hand scale) measured in applied magnetic field 0.1 T parallel to c-axis, (b) temperature dependence of dc-magnetization measured in FC modes with different fields applied parallel to c-axis, (c) temperature dependence of resistivity, with inset showing resistivity on a logarithmic temperature scale, where the solid red line represents fitting to Eq. (1), and (d) temperature dependence of resistivity measured in FC modes with different fields applied parallel to c-axis.

Figure 3 shows the field dependence of the magnetization of $UAu_{0.9}Sb_2$ for fields applied parallel to the c axis at different temperatures. At 50 K, a small plateau with nearly zero magnetization around zero-field can be seen in both up-sweep and down-sweep curves, indicating that the system orders antiferromagnetically at this temperature at zero-field. Two sharp jumps with little hysteresis are observed with magnetic field increasing, i.e., one at around 0.16 T and the other at 1.25 T. These two sharp jumps suggest two metamagnetic transitions appearing. The plateau between 0.16 T and 1.25 T has a magnetization of about one-third of the saturated value, suggesting that this corresponds to a field-induced AFM phase along with an FM component (AFM2). The net magnetization with one-third of the saturated value suggests a magnetic structure along the lines of an 'up–up–down' spin configuration. Above 1.25 T, the magnetization changes little, indicating a spin-polarized phase with a saturated moment of around 1.36 μ_B/U. At 40 K, around zero-field, the small plateau with nearly zero magnetization disappears, while the plateau with the one-third magnetization appears, which suggests that at this temperature the system corresponds to AFM2 phase at zero-field. With increasing field, a field-induced metamagnetic transition occurs at 1.1 T with little hysteresis. At 30 K, the hysteresis at the metamagnetic transition becomes clear and a small hysteresis develops around zero-field, which is consistent with the splitting of the ZFC and FC curves at a slightly higher temperature in Fig. 2(a). At 20 K, the plateau with the one-third magnetization disappears and a number of very small steps appear. This may either signify an additional change of the magnetic structure, or the coexistence of the AFM2 state with small regions of either the AFM or FM phase. At lower temperatures, as shown for example by the curves at 2 K and 15 K, the magnetization remains very near the high-field saturated value upon sweeping down from high fields to zero-field, thereby giving strong evidence for a ferromagnetic ground state.

Figure 4 shows the field dependence of the in-plane resistivity of $UAu_{0.9}Sb_2$ for the applied field along the c axis at different temperatures. The data at 50 K display two sharp drops of the resistivity with increasing field, which is in agreement with the magnetization measurements. At 40 K, only one sharp drop of the resistivity can be observed from zero-field to high field. The resistivity remains nearly the same with the reversed field being around zero-field, indicating that the reorientation of the moment is very fast. At 30 K, an obvious

hysteresis around zero-field in the magnetoresistance develops and the hysteresis at the metamagnetic transition significantly increases, which is in agreement with the magnetization data. At lower temperatures, the hysteresis at the metamagnetic transition in the magnetoresistance can be observed over a broader field range, and disappears only when the moments align in the field-induced FM state. At 2 K, only one drop of the resistivity can be seen in the upsweep curves (from 0 to ±9 T) without any other change with reversed field, indicating a very fast reorientation of the moment in the FM state.

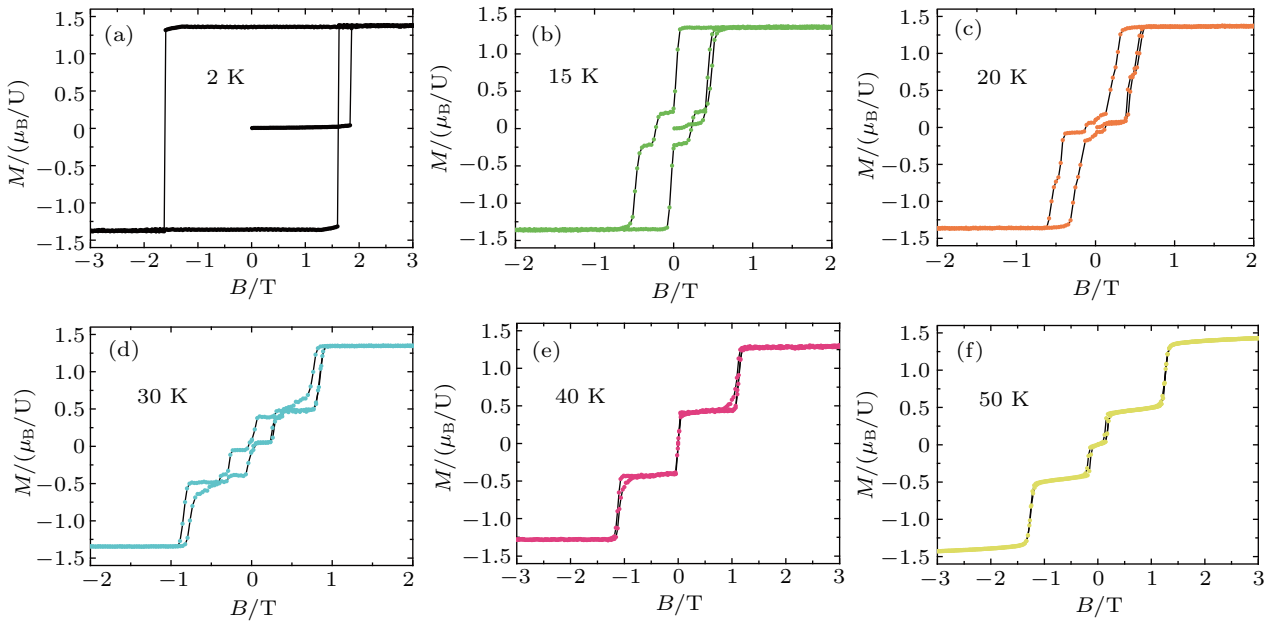


Fig. 3. Plots of magnetization of $UAu_{0.9}Sb_2$ single crystal versus applied magnetic field parallel to the c axis at different temperatures.

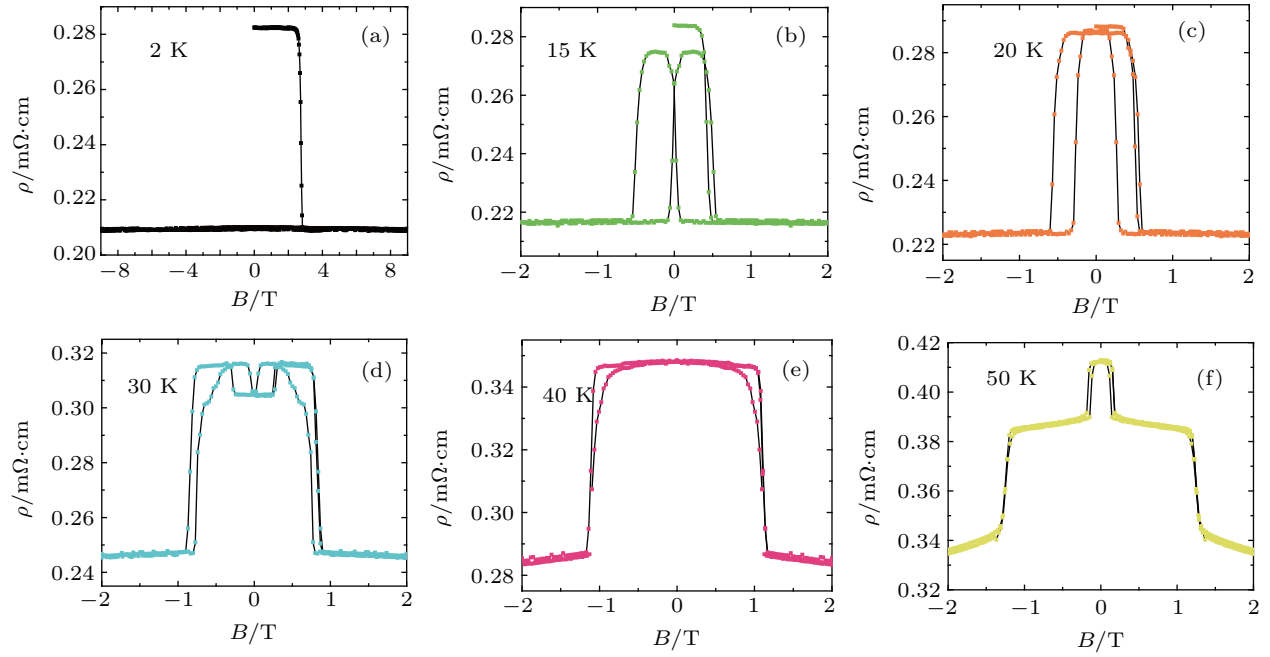


Fig. 4. Plots of in-plane resistivity of $UAu_{0.9}Sb_2$ single crystal versus applied magnetic field along c axis at different temperatures.

Figure 5 shows the field–temperature phase diagram of $UAu_{0.9}Sb_2$ single crystal derived from the resistivity and magnetization data, with an external field applied along the c axis. While those in the upsweep curves (from 0 to ±9 T) may arise from the alignment of magnetic domains, the locations of the transitions are determined from the down-sweep measurements from high fields in this phase diagram. Upon cooling down in zero field, the system undergoes an antiferromagnetic transition to a phase labeled AFM1. Meanwhile, upon increasing the field along the c axis, a metamagnetic transition occurs and the system changes into another antiferromagnetic phase marked as AFM2, which has both antiferromagnetic and fer-

romagnetic components. With further increasing the field, the system transfers into a field induced ferromagnetic state. At lower temperatures, the AFM1 phase is suppressed and the system is in the AFM2 state in zero field, where nearly one-third of the saturated magnetization remains. Upon cooling further, the ground state becomes ferromagnetic, as evidenced by the ferromagnetic-like hysteresis loop in the magnetization. To understand the nature of the magnetic phases and determine the magnetic structure, low temperature neutron diffraction measurements are highly desirable.

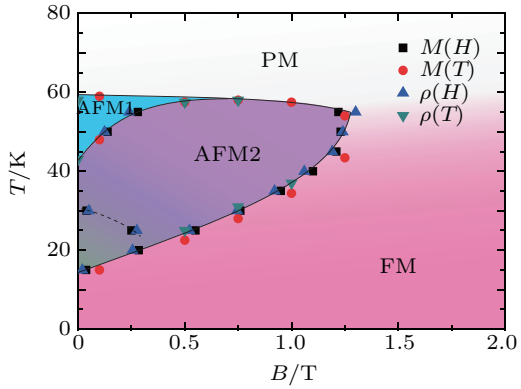


Fig. 5. Field–temperature phase diagram of $UAu_{0.9}Sb_2$ single crystal derived from the resistivity and magnetization data, with an external field applied parallel to the c axis.

Having clearly characterized the physical properties of $UAu_{0.9}Sb_2$, we further study the physical properties of $UAu_{0.75}Sb_2$ by measuring the magnetization and electrical resistivity. Figure 6(a) displays the temperature dependence of dc-magnetization $M(T)$ of $UAu_{0.75}Sb_2$ single crystal. The magnetization curves each still show three features with temperature decreasing: the first feature is a peak feature centered at 95 K which likely corresponds to an antiferromagnetic transition, the second one is a small peak at 47 K which may correspond to another antiferromagnetic magnetic transition, and the third one is the increasing of the magnetization and the splitting of the ZFC and FC curves at lower temperature. Figure 6(b) shows the temperature dependence of the dc-magnetization measured in the FC modes with different fields along the c axis. When increasing the magnetic field, the possible antiferromagnetic transition is gradually suppressed and the ferromagnetic transition temperature increases. The electrical resistivity of $UAu_{0.75}Sb_2$ single crystal displays a maximum value and a Kondo scattering at high temperature as shown in Fig. 6(c). The resistivity at a certain field shows a sudden decrease which is consistent with its magnetization curve from Fig. 6(b). As shown in Figs. 2 and 6, both the magnetization and resistivity of $UAu_{0.75}Sb_2$ disply similar behavior to those of $UAu_{0.9}Sb_2$, while the magnetic transition temperatures are different. A lager composition of Au in $UAu_{1-x}Sb_2$ can suppress the AFM1 transition temperature.

Figure 7 shows the field dependence of the magnetization of $UAu_{0.75}Sb_2$ single crystal for fields applied parallel to the c axis at different temperatures. Its behavior similar to that of $UAu_{0.9}Sb_2$ single crystal can also be detected, such as two metamagnetic transitions at 50 K and 60 K, a small hysteresis developing around zero-field at 25 K, and a ferromagnetic-like hysteresis loop at 2 K. Also some differences can be found between $UAu_{0.75}Sb_2$ and $UAu_{0.9}Sb_2$. One difference is the

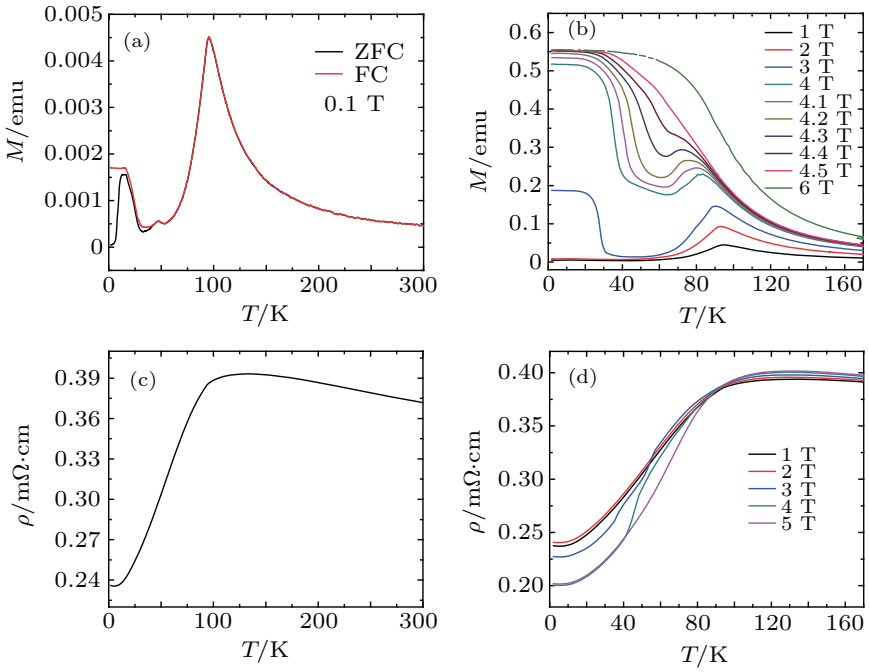


Fig. 6. Plots of dc-magnetization and electrical resistivity of $UAu_{0.75}Sb_2$ single crystal, showing (a) temperature dependence of dc-magnetization $M(T)$ measured in applied magnetic field 0.1 T parallel to c-axis, (b) temperature dependence of dc-magnetization measured in FC modes with different fields applied parallel to c-axis, (c) temperature dependence of resistivity, and (d) temperature dependence of resistivity measured in FC modes with different fields applied parallel to c-axis.

ferromagnetic transition temperature. The onset temperature of $UAu_{0.75}Sb_2$ is around 4 K, where the magnetization remains the high-field saturated value upon sweeping down from high fields to zero-field, and it is around 15 K for $UAu_{0.9}Sb_2$. Thus a lager composition of Au in $UAu_{1-x}Sb_2$ can increase the FM transition temperature. The other difference is the position of the metamagnetic transition. At the same temperature, a lager external field is needed for $UAu_{0.75}Sb_2$ to induce the metamagnetic transitions.

We now combine the magnetic properties of different compositions of Au in $UAu_{1-x}Sb_2$ to discuss the variation of its magnetic properties and the potential quantum critical behavior in this system. The magnetic transition temperatures for different compositions are summarized in Table 1, and figure 8 shows the phase diagram of $UAu_{1-x}Sb_2$ derived from the resistivity and magnetization data, with an external field applied parallel to the c axis. This phase diagram can give a direct insight into the mechanism of the complex magnetism in this system. The USb_2 undergoes only one AFM transition at 203 K[17] and $UAu_{1-x}Sb_2$ undergoes both AFM and FM transitions. Meanwhile, with the increasing of composition of Au, the AFM transition temperature is significantly suppressed and the FM transition temperature increases. This suggests that the magnetic order of $UAu_{1-x}Sb_2$ can be tuned by varying the composition of Au. More occupation of Au site can suppress the antiferromagnetic interactions, reducing T_N, but induces a ferromagnetic transition at lower temperature and lager T_C. Such a complex magnetic order emerging in these compounds may be governed by an interplay between Kondo effect and RKKY exchange modified by crystal-field effects and f–s, f–p, and f–d hybridizations of U with Au and Sb.

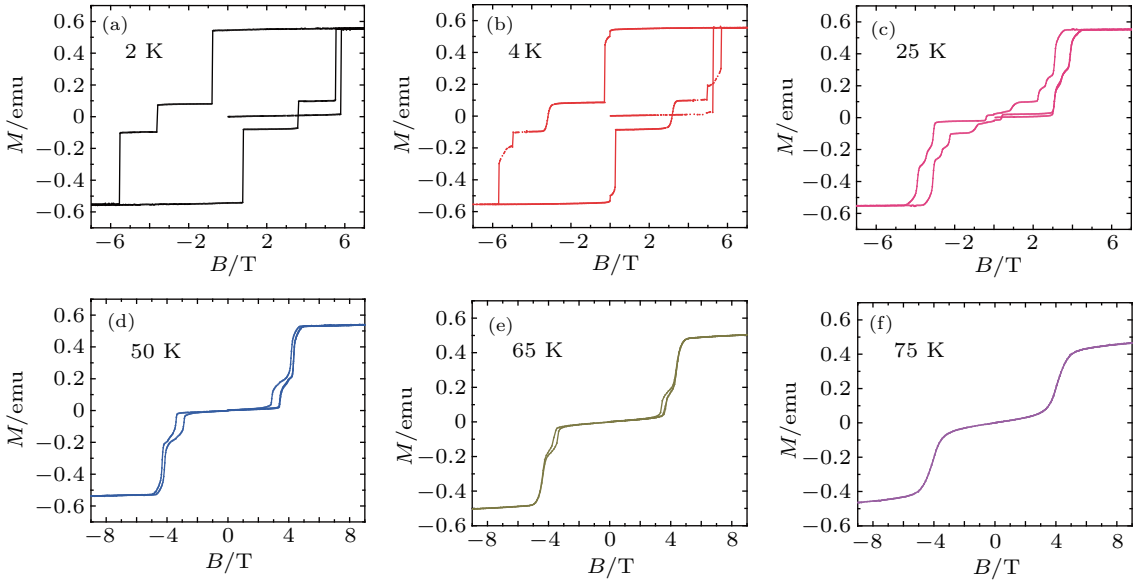


Fig. 7. Plots of in-plane resistivity of $UAu_{0.75}Sb_2$ single crystal versus applied magnetic field along the c axis at different temperatures.

Table 1. Magnetic data for $UAu_{1-x}Sb_2$ compounds.

	USb_2	$UAu_{0.75}Sb_2$	$UAu_{0.8}Sb_2$	$UAu_{0.9}Sb_2$	$UAuSb_2$
T_N/K	203[17]	95	71[19]	59	43[18]
T_C/K	–	4	10[19]	15	31[18]

Full occupation of Au site suppresses the AFM transition temperature to 43 K in $UAuSb_2$.[18] With reducing the occupation of Au site, the FM transition temperature decreases and reaches 4 K in $UAu_{0.75}Sb_2$ and disappears in USb_2, which suggests a potential quantum critical point existing between the compositions. Thus reducing the occupations of Au site is possible to suppress the FM transition temperature to zero and a potential quantum critical point may emerge in $UAu_{1-x}Sb_2$. Therefore it is of great interest to study more nonstoichiometric $UAu_{1-x}Sb_2$ compounds between $x = 1$ and 0.25 to examine the potential quantum critical behavior in this system.

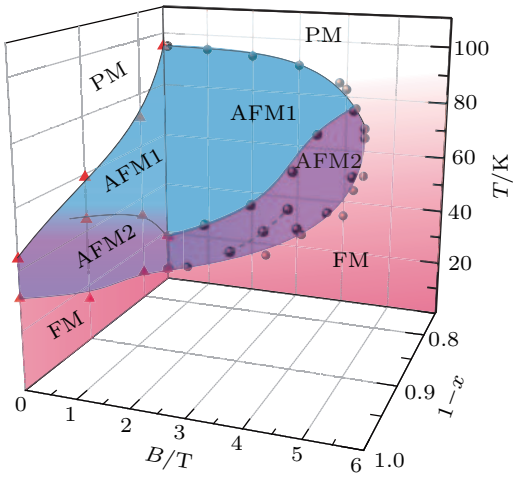


Fig. 8. Phase diagram of $UAu_{1-x}Sb_2$ derived from resistivity and magnetization data, with an external field applied parallel to the c axis.

4. Conclusions

We have successfully synthesized two nonstoichiometric $UAu_{1-x}Sb_2$ single crystals and performed a detailed investigation of their physical properties. Three magnetic phases are evidenced by magnetization and electrical resistivity measurements: a high temperature antiferromagnetic phase, a phase with both ferromagnetic and antiferromagnetic components at intermediate temperatures, and a low temperature ferromagnetic phase. Two metamagnetic transitions are found with an external field applied parallel to the c axis in this system. The magnetic order can be tuned by varying the occupation of Au site. With increasing the occupation of Au site, the AFM transition temperature is significantly suppressed and the FM transition temperature increases. A potential quantum critical point is possible for less occupation of Au site and more further work is needed to examine the potential quantum critical behavior in this system.

Acknowledgment

We thank Chunli Jiang for technical assistance with EDS measurements.

References

[1] Stewart G R 1984 *Rev. Mod. Phys.* **56** 755
[2] Santini P, Lémanski R and Erdős P 1999 *Adv. Phys.* **48** 537
[3] Palstra T T M, Menovsky A A, van den Berg J, Dirkmaat A J, Kes P H, Nieuwenhuys G J and Mydosh J A 1985 *Phys. Rev. Lett.* **55** 2727
[4] Maple M B, Chen J W, Dalichaouch Y, Kohara T, Rossel C, Torikachvili M S, McElfresh M W and Thompson J D 1986 *Phys. Rev. Lett.* **56** 185
[5] Broholm C, Kjems J K, Buyers W J L, Matthews P, Palstra T T M, Menovsky A A and Mydosh J A 1987 *Phys. Rev. Lett.* **58** 1467
[6] Shang T, Chen Y H, Jiang W B, Chen Y, Jiao L, Zhang J L, Weng Z F, Lu X and Yuan H Q 2014 *J. Phys. Condens. Matter* **26** 045601
[7] Yuan H Q, Grosche F M, Deppe M, Geibel C, Sparn G and Steglich F 2003 *Scinece* **302** 2104
[8] Si Q M and Steglich F 2010 *Scinece* **329** 1161
[9] Saxena S S, Agarwal P, Ahilan K, Grosche F M, Haselwimmer R K W, Steiner M J, Pugh E, Walker I R, Julian S R, Monthoux P, Lonzarich G G, Huxley A, Sheikin I, Braithwaite D and Flouquet J 2000 *Nature* **406** 587
[10] Kaczorowski D, Kruk R, Sanchez J P, Malaman B and Wastin F 1998 *Phys. Rev. B* **58** 9227
[11] Kaczorowski D 1992 *J. Alloys Compds.* **186** 333
[12] Bukowski Z, Kaczorowski D, Stęgpień-Damm J, Badurski D and Troć R 2004 *Intermetallics* **12** 1381
[13] Torikachvili M S, Davis B K, Kothapalli K, Nakotte H, Schultz A J, Mun E D and Bud'ko S L 2011 *Phys. Rev. B* **84** 205114
[14] Bukowski Z, Tran V H, Stęgpień-Damm J and Troć R 2004 *J. Sol. State. Chem.* **177** 3934
[15] Bukowski Z, Troć R, Stępień-Damm J, Sułkowski C and Tran V H 2005 *J. Alloys Compds.* **403** 65
[16] Bobev S, Mixson D J, Bauer E D and Sarrao J L 2006 *Acta Crystallogr. Sect. E* **62** i64
[17] Leciejewicz J, Troć R, Murasik A and Zygmunt A 1967 *Phys. Stat. Sol.* **22** 517
[18] Troć R, Bukowski Z, Stępień-Damm J and Sułkowski C 2009 *Acta Phys. Pol. A* **115** 181
[19] Zhang W, Guo C Y, Xie D H, Smidman M, Hu B F, Xia Y H, Liu Y, Tan S Y, Feng W, Zhu X G, Zhang Y, Hao Q Q, Luo L Z, Yuan H Q and Lai X C 2018 *Sci. Rep.* **8** 7835